Article:
Almatouq, A and Babatunde, AO (2017) Concurrent Hydrogen Production and Phosphorus Recovery in Dual Chamber Microbial Electrolysis Cell. Bioresource Technology, 237. pp. 193-203. ISSN: 0960-8524

https://doi.org/10.1016/j.biortech.2017.02.043

Concurrent Hydrogen Production and Phosphorus Recovery in Dual Chamber Microbial Electrolysis Cell

Abdullah Almatouq, A.O. Babatunde

PII: S0960-8524(17)30160-8
DOI: http://dx.doi.org/10.1016/j.biortech.2017.02.043
Reference: BITE 17615

To appear in: *Bioresource Technology*

Received Date: 12 December 2016
Revised Date: 8 February 2017
Accepted Date: 12 February 2017

Please cite this article as: Almatouq, A., Babatunde, A.O., Concurrent Hydrogen Production and Phosphorus Recovery in Dual Chamber Microbial Electrolysis Cell, *Bioresource Technology* (2017), doi: http://dx.doi.org/10.1016/j.biortech.2017.02.043

Concurrent Hydrogen Production and Phosphorus Recovery in Dual Chamber Microbial Electrolysis Cell

Abdullah Almatouq [1,2]*, and A. O. Babatunde[3]

[1] Hydro-Environment Research Centre, Energy and Environment Theme,
Cardiff University School of Engineering, Queen's Buildings, The Parade, Cardiff CF24 3AA, UK;

[2] Kuwait Institute of Scientific Research, P.O. Box 24885, Safat 13109, Kuwait

[3] Institute of Public Health and Environmental Engineering, School of Civil Engineering, University of Leeds, Leeds LS2 9JT, UK

* Correspondence: amatouq@kisr.edu.kw; Tel.: +44-29-2087-0076; Fax: +44-29-2087-4939

Abstract

Concurrent hydrogen (H_2) production and phosphorus (P) recovery were investigated in dual chamber microbial electrolysis cells (MECs). The aim of the study was to explore and understand the influence of applied voltage and influent COD concentration on concurrent H_2 production and P recovery in MEC. P was efficiently precipitated at the cathode chamber and the precipitated crystals were verified as struvite, using X-ray diffraction and scanning electron microscopy analysis. The maximum P precipitation efficiency achieved by the MEC was 95%, and the maximum H_2 production rate was 0.28 m^3-H_2/m^3-d. Response surface methodology showed that applied voltage had a great influence on H_2 production and P recovery, while influent COD concentration had a significant effect on P recovery only. The overall energy recovery in the MEC was low and ranged from 25 ± 1 to 37 ± 1.7 %. These results confirmed MECs capability for concurrent H_2 production and P recovery.

Keywords: Bio-electrochemical System; Phosphorus Recovery; Microbial Electrolysis Cell; Struvite; Response Surface Methodology

1.0 Introduction

Due to population growth, the global demand for unsustainable resources is rising. As a result, concerns around resource depletion are increasing. Phosphorus is one of the most

important unsustainable nutrients on our planet. Phosphorus is essential for all forms of life, especially for plant growth. Unfortunately, estimates show that phosphorus rocks will be depleted within the next 50-100 years (Cooper et al., 2011). Therefore, alternative sources of phosphorus should be discovered to balance the high demand for phosphorus. Magnesium ammonium phosphate (struvite) is one of most common phosphate fertilizers that can be recovered from different streams of wastewater. Struvite is an efficient slow release fertilizer that can be used for crop growth, and is an excellent alternative for phosphate rocks (Rahman et al., 2014).

Struvite precipitation occurs in the equimolecular concentration of magnesium (Mg), ammonium (NH_4) and (P); these elements combine with water to form struvite. The precipitation of these components is also highly dependent on pH, where struvite starts to precipitate at pH > 8 (Doyle & Parsons, 2002). The most common methods for P recovery as struvite are chemical addition and carbon dioxide stripping through aeration. These processes are effective for struvite precipitation; however, the operation cost is too high. Using chemical addition to raise the solution's pH can account for up to 97% of struvite cost (Jaffer et al., 2002; Morales et al., 2013).

Microbial electrolysis cells (MECs) are a new and promising approach for hydrogen (H_2) production from organic matter, including wastewater and other renewable resources. In MECs, electrochemically active bacteria oxidise organic matter and generate CO_2, electrons and protons. The bacteria transfer the electrons to the anode and the protons are released into the solution. The electrons then travel through a wire to a cathode and combine with the free protons in the solution to produce hydrogen gas (Equations [1] and [2]) (Logan et al., 2008).

Anode chamber: $CH_3COO^- + 4\ H_2O \rightarrow 2\ HCO^{3-} + 9\ H^+ + 8\ e^-$ (1)

Cathode chamber: $8\ H^+ + 8\ e^- \rightarrow 4\ H_2$ (2)

The consumption of protons at the cathode chamber increases solution pH (Moussa et al., 2006). Based on this hypothesis, the cathode chamber in the MEC can be used to precipitate P as struvite.

MECs have been used for different applications such as hydrogen production (Call & Logan, 2008), methane production (Ding et al., 2016), ammonium recovery (Kuntke et al., 2014) and P recovery (Cusick & Logan, 2012; Cusick et al., 2014). The recovery of P in MEC has not been studied in depth; few studies have focused on the topic to date. Single chamber microbial electrolysis cells were used to recover P as struvite via synthetic anaerobic digestion from a domestic wastewater treatment plant (Cusick & Logan, 2012). In this study, two types of cathode (stainless steel mesh and flat plate) were used to identify the impact of cathode type on P removal. The single chamber MEC achieved a maximum P removal of 40% with a stainless steel mesh cathode, and there was no crystal accumulation effect on hydrogen production. In terms of H_2 production, the MEC achieved a maximum H_2 production rate of 2.3 m^3-H_2/m^3-d. The applied voltage did have an effect on hydrogen production, and on the rate of struvite crystallization.

The accumulation of protons and hydroxide ions in the same electrolyte in single chamber MEC led to the buffering of the pH, therefore low P recovery in the single chamber MEC was observed. A dual chamber MEC with a fluidized bed cathode was suggested to enhance P removal. A dual chamber MEC has better separation between the anode and cathode, which helps induce pH increases in the cathode chamber (Cusick et al., 2014). A fluidized bed cathode was used to inhibit scale formation on the cathode surface. The MEC achieved a maximum P removal of 85%, and the precipitates were shown to be struvite. However, the study focused only on P recovery and did not study hydrogen production. Therefore, a

comprehensive study should be conducted to assess MEC performance for concurrent H_2 production and P recovery.

In this study, a dual chamber MEC was used to overcome the pH buffering between the anode and the cathode. In addition, both hydrogen production and P recovery have been studied to assess MEC performance. The main aim of this study was to understand the influence of applied voltage and COD concentration on hydrogen production and struvite crystallization. The specific objectives of the study were: (i) to understand the role of applied voltage and COD concentration in P recovery as struvite and in H_2 production using a dual-chamber MEC; and (ii) to improve and optimize struvite precipitation and hydrogen production under different operational conditions (applied voltage and COD concentration), using a response surface methodology (RSM) optimization statistical model.

2.0 Materials and Methods

2.1. Reactor Set-up and Inoculation

Two sets of dual-chamber H-type bottles (Adams & Chittenden Scientific Glass, Berkeley, CA, USA), were used to construct the MECs (Figure 1). Each set contained two identical bottles with a volume of 300 mL for each chamber. The anode and cathode electrodes were made of carbon cloth measuring 2.5 × 5 cm, with a projected area of 25 cm^2 (Fuel Cells Etc, Texas, USA). The cathode contained a Pt catalyst (0.5 mg/cm^2 10% Pt on carbon cloth electrode) to improve cathode performance, whilst the anode was plain carbon cloth. Both electrodes were connected with a titanium wire (0.5 mm, purity > 99.98%, Alfa Aesar, Heysham, UK). A Nafion membrane (Nafion 117#, Sigma-Aldrich, London, UK), with an area of 12.57 cm^2, was placed in the middle of the anode and the cathode chambers. The membrane was pretreated by boiling in H_2O_2 (30%) and deionized water, followed by 0.5 M H_2SO_4 and deionized water, each for one hour. It was then stored in deionized water

prior to being used. A DC power supply PSD 30/3B (CALTEK, Hong Kong) was used to apply voltage for the MEC. The voltage was added by connecting the positive pole of the power source to the anodes while the negative pole led to a high precision resistor (10 Ω) and the cathodes. The anode chamber was inoculated with a 1:1 mixture of activated sludge and anolyte medium (containing in (g/L): Sodium acetate 3.28 + ammonium chloride 0.31+ potassium chloride 0.13 + sodium phosphate anhydrous monobasic 2.69 + disodium hydrogen phosphate 4.33 + 10 mL of vitamins solution + 10 mL of a trace element solution). The cathode chamber was filled with 50 mM phosphorus buffer, and it was continuously aerated using an aquarium pump. Both electrodes were connected to 1000 Ω of external resistance at the initial stage of the operation; this was changed to 10 Ω after the inoculation process. A fresh medium combined with inoculum mixture was used to replace the anolyte, when the voltage dropped.

2.2 MEC Experimental Design

Anode synthetic wastewater contained (0.5-2 g/L depends on the COD concentration used); Sodium acetate; KH_2PO_4, 0.65 g/L; K_2HPO_4, 0.65 g/L; KCl, 0.74 g/L; NaCl, 0.58 g/L; NH_4Cl, 0.375 g/L; $MgSO_4 \cdot 7H_2O$, 0.1 g/L; $CaCl_2 \cdot 2H_2O$, 0.1 g/L; 0.1 mL/L of a trace element mixture and vitamins. The cathode synthetic wastewater contained (0.5 g/L sodium acetate; KH_2PO_4, 0.25 g/L; K_2HPO_4, 0.25 g/L; KCl, 0.74 g/L; NaCl, 0.58 g/L; NH_4Cl, 0.375 g/L; MgCl2, 0.32 g/L; $MgSO_4 \cdot 7H_2O$, 0.1 g/L; $CaCl_2 \cdot 2H_2O$, 0.1 g/L). Anode and cathode influent pH were adjusted to pH = 7. After each MEC cycle, the anode chamber was drained, and exposed to air for 30-45 minutes to inhibit methanogen growth (Call & Logan, 2008). It was then, refilled with synthetic wastewater solution, and both anode and cathode chambers were sparged for 20 minutes with pure N_2. The MECs were run at applied voltages (of 0.4, 0.5, 0.8, 1.1 and 1.2 V) for at least three batch cycles at each voltage. In addition, five COD levels

were used in the anode feed solution as follows: 300, 500, 1000, 1500 and 1700 mg/L. The current densities and operation time of a cycle varied with the changes in anolyte compositions. The COD consumption was calculated at the end of each cycle using DR3900 Spectrophotometer (HACH, UK). The volume of the produced gas in the cathode chamber was measured via the displacement method. Anolyte and catholyte pH and oxidation-reduction potential (ORP) were measured continuously every 15 minutes during each batch using 12-Channel measuring and monitoring data logger (EA Instruments, London, UK).

2.3 Analytical Methods

The voltage across the external resistance was recorded every 15 minutes using the ADC-20 data logger system (Pico Technology, UK). Current was calculated using Ohm's law by measuring the voltage across a resistor (10Ω). Hydrogen production rate (m^3-H_2/m^3-d), coulombic efficiency (CE), the amount of energy added to the MEC by the power source (W_E), the amount of energy added by the substrate (W_s) energy efficiency (η_E), and overall system efficiency (η_{E+S}) were calculated as previously described (Logan et al., 2008). In addition, the electrical energy input and the electrical energy recoverd were calcultated using eq. (3&4):

- The electrical energy input per kg of COD removed (Wh_{in}/kg-COD)

$$Wh_{H2} = \frac{\int_2^t W_{in} dt}{\Delta COD.V} \quad (3)$$

where W_{in} is the electrical input, ΔCOD the change in solution COD, and V the reactor liquid volume.

- The energy recovered as hydrogen per kg of COD (Wh_{H2}, kWh/kg-COD)

$$Wh_{H2} = Y_{H2}.HHV_{H2} \quad (4)$$

where Y_{H2}(kg H_2/kg-COD) is the hydrogen yield, HHV_{H2} is the higher heating value of hydrogen (39.4 kWh/kg-H_2)

2.4 Water Analysis

All results reported are the average of at least six independent trials (three cycles for each cell). Chemical oxygen demand (COD), ammonium (NH_4-N), orthophosphate (PO_4^{-3}) concentrations were measured after each cycle. Total phosphorus (TP), magnesium (Mg), calcium (Ca), potassium (K), and sodium (Na) concentration were measured using inductively coupled plasma optical emission spectrometry (ICP-OES).

2.5 Gas Analysis

The total volume of the gas produced was measured using the water displacement method (Logan et al., 2008). A gas chromatograph (compact GC, CE Instruments Ltd, UK) was used to analyze the produced gas in the cathode chamber during each batch, but anode gases were analysed periodically. The compact GC was equipped with a thermal conductivity detector (TCD) and Flame ionization detector (FID). Argon gas was used as a carrier gas for the GC.

2.6 Phosphorus Precipitation in MEC

The theoretical P, Mg, and NH_4 concentrations in the cathode solution were approximately 3 mM at pH 7. For P precipitation as struvite a 1:1:1 molar ratio of NH_4:Mg:P should be achieved (Doyle & Parsons, 2002). Before and after each cycle, the cathode chamber was washed with deionised water three times, and then cleaned and dried properly to remove any attached precipitates on the chamber walls. After each precipitation cycle, the used cathode was removed for maintenance and was replaced with new electrode. Cathode maintenance is essential to remove P precipitates from cathode surface, as the precipitates reduce cathode performance and dissolution treatment increases cathode performance to their initial level. The electrode was immersed 3 times in deionised water (pH=7) for 2 days each time. After deionized water dissolution, the electrode was immersed again 3 times in MES buffer ($C_6H_{13}NO_4S$ [MES]:10 mM, adjusted to pH 5.5 with NaOH) each time for 30 hours. Finally,

the electrode was rinsed and dried before use. At the end of each cycle, the catholyte was filtered using a 0.2 um filter membrane (Fisher Scientific, UK). The precipitate was collected, weighed and analysed by X-ray diffraction (XRD) and by scanning electron microscopy coupled with energy dispersive X-ray spectroscopy (SEM-EDS). The recovered P was calculated using Equation (5):

$$\text{Precipitation efficiency } (\%) = \frac{P_{in} - P_{out}}{P_{in}} \times 100 \quad (5)$$

where P_{in} = P concentration in the catholyte influent, P_{out} = P concentration in the catholyte effluent. In addition, P precipitation rate (g-P/$m^3_{cathode}$-d) was calculated using Equation (6):

$$\text{P precipitation rate (g-P/m}^3_{\text{cathode}}\text{-d)} = \frac{(TP_{in} - TP_{out}) \times V_{catholyte}}{V_{cathode} \times \Delta t} \quad (6)$$

where TP_{in}= total phosphorus influent cathode concentration, TP_{out}= total phosphorus effluent cathode concentration, $V_{catholyte}$ = volume of catholyte solution (m^3), $V_{cathode}$ = volume of cathode chamber (m^3), and Δt= batch duration (d).

2.7 Scanning Electron Microscopy (SEM) and Energy Dispersive X-ray Spectrometry (EDX) Analysis

For SEM analysis, the precipitates that accumulated on the cathodes and in the cathode chamber were analyzed to examine the morphology of the crystal as well as its elemental composition. In addition, the used proton exchange membrane (PEM) was cut into pieces, carefully rinsed with deionized water and finally dried completely at ambient temperature. The microscopic structure and elemental components of the PEM surface were analyzed using a FEI-XL30 Environmental SEM equipped with an EDX.

2.8 Crystals Composition and Purity

The purity of the collected crystals was determined by analysing crystals composition. Struvite purity was determined using SEM-EDS and the dissolution method to identify the composition of the crystals. Approximately 0.05 g of crystals were dissolved in 50 mL of 0.5% nitric acid solution. In order to accelerate dissolution, the samples were stirred with a magnetic stirrer for 24 hours, after which samples were analyzed for magnesium, ammonia, orthophosphate, calcium, aluminum and iron using inductive coupled plasma (ICP) (Fattah et al., 2008).

2.9 Visual Minteq Software

Visual Minteq modeling software (Visual MINTEQ 3.1) is a chemical equilibrium compouter programme that allows for the calculation of speciation, solubility and equilibrium in both solid and dissolved phases of minerals in an aqueous solution (Çelen et al., 2007). Minteq model default values were used in this study. Minteq was used to predict the saturation index of the soluble salts and oversaturated solids were allowed to precipitate.

2.10 Statistical Analysis

Response surface methodology (RSM) is an efficient statistical tool that helps in understanding and optimising the system by identifying the impact of different parameters on the response. Design Expert Version 10.0.3 (Stat-Ease Inc., Minneapolis, MN, USA) was used for the design, analysis, and optimisation. The used parameters were: applied voltage (X1) and influent COD concentration (X2). The responses were: cathode pH (Y1), Precipitation efficiency (Y2), and maximum volumetric hydrogen production (Y3). Analysis of variance (ANOVA) provided the statistical results and the diagnostic check tests to evaluate the adequacy of the models. The quality of the fitted models was evaluated using the

coefficient of determination R^2, and its statistical significance was checked by the Fisher F-test. Model terms were evaluated by the P-value (probability of error) with 95% confidence level. Three-dimensional plots and their respective contour plots were obtained based on the effects of the two factors (applied voltage and COD). In total, 19 experiments were conducted with 8 factorial points, 8 axial points, and 3 center point. Replicates of the center points were added to the design to examine the adequacy of the model and to get a good estimate of the experimental error.

2.10.1 Central Composite Design (CCD)

The study determined the effects of applied voltage (X_1) and influent COD concentration (X_2) on cathode pH, precipitation efficiency and maximum volumetric hydrogen production. The nonlinear behavior of the response is explained by the following quadratic model:

$$y = \beta_o + \sum_{I=1}^{n} \beta_i Xi + \sum_{i=1}^{n} \beta_{ii} X_i^2 + \sum_{i=1}^{n-1} \sum_{j=1+i}^{n} \beta ij\, X_i X_j + E \quad (7)$$

where y is the response, βi is the coefficient of the ith main effect, β_{ii} is the coefficient of the ith quadratic term, βij is the coefficient of the interaction between the ith and jth terms and E is the error term. Two replicates were employed at each factor combination. At the beginning of each factor combination, the system was run for at least 2 batches to let the system adapt to the new conditions.

3.0 Results and Discussion

3.1 Hydrogen Production

The gases produced in the cathode chamber were analyzed using compact GC; they were found to contain mainly hydrogen in all cases, and methane was detected in the anode chamber. The hydrogen production rate in the dual chamber MEC ranged from 0.06 to 0.28 m^3-H_2/m^3-d. The volume of the produced gas was variable and totally dependent on the applied voltage. Increasing the applied voltage led to an increase in the current density. As a

result, an increase in the production of hydrogen gas ($P < 0.05$) was observed (Figure 2-a). An increase in applied voltage from 0.4 to 1.2 V led to a more than four-fold increase in hydrogen production. The system achieved a maximum volumetric hydrogen production rate of 0.22 ± 0.06 m^3-H_2/m^3-d at (COD=1000 mg/L, applied voltage =1.2).

In addition, different COD concentrations were used to identify the impact of COD concentration on hydrogen production. The cycle duration and the current densities varied when anolyte COD concentrations were changed. There was no correlation between COD concentration and hydrogen production rate, where increasing COD concentration from 300 to 1700 mg/L had no impact on hydrogen production ($P > 0.05$). This means that changing the anolyte COD concentration did not affect the H_2 production rate in the MEC. The maximum hydrogen production rate 0.18 m^3-H_2/m^3-d was achieved at (COD= 500 mg/L, applied voltage = 0.8 V), and the H_2 production rate varied at different COD concentrations. The low hydrogen production rate in this study was similar to previous studies using dual chamber MEC (Ruiz et al., 2015; Yossan et al., 2013), where the maximum H_2 production rate was 0.2 and 0.5 m^3-H_2/m^3-d, respectively. In addition, low H_2 production rate (114.46 ± 3.75 mL/m2) was also observed in single chamber MEC (Pasupuleti et al., 2015).

The overall energy recovery rates in the MEC ranged from $\eta_{E+S} = 25 \pm 1$ to 37 ± 1.7 %. Overall energy recovery was calculated under different applied voltages. The results showed that there is no correlation between applied voltage and overall energy recovery ($P > 0.05$). The electrical consumption in the MEC was higher than the energy production in all tests. An increase in applied voltage in the circuit, from 0.4 to 1.2 V, increased electrical energy input Wh_{in} from 0.5 ± 0.05 to 1.9 ± 0.2 kWh/kg-COD. The low H_2 production in the MEC was not enough to recover the electrical consumption. However, the recovered energy and struvite can be used to reduce the operational cost.

3.2 Phosphorus Recovery in MEC

Phosphorus started to precipitate as struvite when the cathode pH reached 8. The system achieved a maximum precipitation efficiency of 95 ± 2.13%. P was recovered in the cathode chamber, where proton consumption converts the neutral solution to alkaline. Similar results were reported by (Cusick et al., 2014; You et al., 2015), where high P removal was achieved by MEC (85 %) and MFC (82 %), respectively. Cathode pH was affected by applied voltage; an increase in applied voltage from 0.4 to 0.8 V increased the average cathode pH from 8 to 9.1. However, increasing the applied voltage to 1.2 led to a decrease in the average cathode pH, down to 8.5. Using high voltage may inhibit bacteria activity and affect the oxidation process in the anode chamber, with the result that low protons are released and cathode pH is affected.

To understand the role of the current on P recovery and cathode pH, the system was shifted to an open circuit system (OCV), where no resistance was used in the circuit, and MECs were operated for at least three cycles. Cathode pH did not increase and remained at 7. These findings show the importance of determining the ideal applied voltage to obtain high pH in the cathode. Precipitation efficiency (in OCV) was less than 1%, but when the circuit closed and 0.4 V was applied, the MEC achieved 45 ± 5% precipitation efficiency (Figure 2-b). Furthermore, precipitation efficiency improved and reached 90 ± 7% when the applied voltage increased to 0.8 V. At 1.2 V, precipitation efficiency reached 92 ± 5%. The precipitated P was found on the cathode electrode, suspended on the catholyte and on the chamber walls. The precipitation rate achieved in the MECs ranged from 1.4 to 20 g-P/m^3.d. The highest precipitation rate was achieved at 0.8 V. An increase in the applied voltage to 1.2 V decreased the precipitation rate. Increasing the applied voltage to 1.2 V inhibits microorganism activity and increases the cycle duration. The precipitation rate was affected by cycle duration, which decreased with applied voltage (Cusick & Logan, 2012).

The concentrations of P and Mg in cathode influent were approximately 3 mm, and struvite precipitates when the molar ratio of NH_4:Mg:P in the solution is 1:1:1 at an alkaline environment (pH > 8). Figure 3(a-b) show that (in OCV) there was no P removed from the cathode due to a neutral environment (pH=7). This confirms that P was removed only by precipitation. However, more than 1 ± 0.2 mm of Mg was transferred from the cathode chamber to the anode chamber through Nafion membrane exchange, due to the concentration gradient. When 0.4 V was applied to the circuit, catholyte pH increased to 8, and around 1.45 ± 0.2 mm of P and approximately 1.3 ± 0.2 mm of Mg were recovered as struvite. An additional 1 ± 0.1 mm of Mg were transferred from the cathode to the anode. Increasing the applied voltage increased the pH. As a result, the precipitated P and Mg increased. This reduced the Mg transferred to the anode, because most of the Mg was precipitated as struvite. Creating the optimal pH in the cathode chamber is very important, to minimize the diffusion of cations to the anode chamber.

On the other hand, NH_4 concentration in the anode chamber decreased in all cycles due to NH_4 diffusion and microorganism consumption. In addition, NH_4 removal was observed to increase when applied voltage was increased, ranging from 0.7 ± 0.1 mm at 0.4 V to 2.25 ± 0.2 mm at 1.2 V. However, calculating NH_4 concentration in the cathode effluent was challenging. The concentration of NH_4 in the cathode effluent varied and fluctuated in each cycle, due to ammonia volatilization caused by the high pH (Cusick et al., 2014).

3.3 Crystals Analysis

After each batch, the catholyte was filtered and the precipitated crystals were weighed and analyzed. In addition, the cathode electrode was treated, using the dissolution method, and replaced with a new cathode electrode for the next cycle. The XRD pattern showed that the precipitated crystals matched the standard pattern. The SEM images showed that the crystals

had tubular morphology with sharp edges (needle), which confirms that the precipitated crystals were struvite (Hutnik et al., 2011). Furthermore, EDS analysis showed that the main peaks of the crystals (from all cycles) were Mg, O, and P, which are similar to the peaks of struvite standard (Ronteltap et al., 2010). The dissolution treatment for the cathode showed that the molar ratio of Mg:P in the solution was approximately 1:1. This can also confirm that the precipitated crystals had a similar molar ratio to the struvite standard.

On the other hand, Visual Minteq software was used to gain a better understanding of P precipitation in MECs. The main aim behind the Minteq modeling is to understand when P started to precipitate. The concentration of each element in the cathode synthetic influent solution was added to the software. The model result showed that 5 different minerals were formed: Hydroxyapatite, tricalcium phosphate, octacalcium phosphate, bobierrite and struvite. However, hydroxyapatite was eliminated because magnesium ions in the solution kinetically obstruct the nucleation and formation of this species. In addition, octacalcium was eliminated because it formed at low pH (5-6) (Çelen et al., 2007).

The SEM and XRD analysis showed that only struvite was precipitated in the cathode chamber. The model showed that struvite started to be supersaturated when the cathode pH reached 8.1. In the supersaturated solution, P started to precipitate as struvite. The model confirms the experimental results; struvite started to precipitate when the cathode pH reached 8.

3.4 Cathode and Membrane Scaling

A deterioration in the current was observed during the time of operation. The more precipitates on the cathode surface, the more fluctuation in the current was noticed. At 1.2 V, the electrode was completely covered with struvite and the current started to drop after one day of operation, and this continued until the end of the batch duration. No deterioration in

current (in OCV) was noticed, which confirms the effect of P recovery on the current. Similar findings were observed in previous studies (Almatouq & Babatunde, 2016; Cusick et al., 2014). After each cycle, the cathode electrode was replaced with a new electrode and the used electrode was removed for maintenance. The electrode was immersed in the MES solution to remove any P precipitates on its surface. Through dissolution processes, the P concentration was measured to quantify the concentration of P on the cathode electrode. Due to the high pH around the cathode electrode, more than 50% of P was precipitated on the electrode surface.

Furthermore, after a long-term operation, the PEM in MECs was affected by the precipitates. PEM is another important factor that has an impact on MEC performance, where the membrane resistance contributes to the total internal resistance of MEC. Therefore, membrane fouling and an increase in membrane resistance can also lead to deteriorated MEC performance (Xu et al., 2012).

SEM and EDS analysis were used to identify the impact of P precipitation on the membrane. SEM pictures showed that the surface of the new PEM was smooth and clear, without any particles on the surface, and that the main components of the new PEM were oxygen, carbon, fluoride and sulfur (Çetinkaya et al., 2015). In contrast, the SEM image of the used PEM contained many small particles with different shapes on the surface. The EDX analysis showed that the PEM contains phosphorus, magnesium and calcium precipitations, which were mainly precipitated during the operation time. These results confirmed that some of the struvite particles were attached to the PEM surface. The precipitation of these particles and salts during the long-term operation of MECs would deteriorate the MECs' performance and increase internal resistance.

3.5 COD Removal Efficiency and Water Analysis in the Anode

COD removal is an important parameter to assess the ability of MECs to treat wastewater and to find any correlation between applied voltage and COD removal. MECs were operated under different applied voltages (0.4, 0.5, 0.8, 1.1, and 1.2) at COD =1000 mg/L. The achieved COD removal efficiency ranged from 59 to 92%. COD removal efficiency increased when the applied voltage was increased from 0.4 to 0.8 V, where the system achieved the maximum removal efficiency. The removal efficiency then decreased when the applied voltage rose above 0.8 V. Increasing the applied voltage from 0.4 V to 0.8 V increased the removal efficiency by 30%. In addition, increasing the applied voltage above 0.8V had a negative impact on COD removal, where high voltage could inhibit bacteria activity. As a result, low COD removal was observed (Ding et al., 2016). Similar results, with high COD removal efficiency, were found in dual chamber MEC (Ding et al., 2016). It was shown that the applied voltage had a great impact on COD removal and that applying the optimal value can improve COD removal and reduce the operational cost.

Furthermore, MECs were operated under different COD concentrations (300, 500, 1000, 1500 and 1700) at applied voltage = 0.8 V. The achieved COD removal efficiency ranged from 50 to 90%. High COD removal was achieved with low influent COD concentration. High influent COD concentration requires long batch cycles, where the bacteria needs more time to degrade the organic matter. The results showed that COD removal was clearly affected by current generation and by the period of a batch cycle.

On the other hand, water quality parameters (NH_4^+, NO_3^-, NO_2^- and TP) were analyzed in the influent and effluent of the anode chamber. The concentration of $N\text{-}NH^{4+}$ and TP in the anode influent were 94.5 ± 2.9 and 100 ± 7 mg/L, respectively. The concentration of TP in the anode effluent was 102 ± 2.7 mg/L. TP concentration in the anode effluent was equal to or

slightly higher than that in the anode influent, due to the release of stored phosphate in the bacteria under an anaerobic environment (Tao et al., 2014). The concentration of N-NH^{4+} in the anode effluent was 65 ± 10 mg/L. The reduction of ammonium concentration in the anolyte occurred due to microbial consumption and ammonium diffusion to the cathode chamber through Nafion 117, to compensate charge balances between the anode and cathode chambers (concentration gradient) (Cord-Ruwisch et al., 2011). Moreover, the concentrations of nitrate and nitrite in the anode effluent were low and nearly the same as those in the anode influent, due to the anaerobic environment.

3.6 Coulombic Efficiency (CE)

The achieved coulombic efficiency ranged from 8 to 51 %. CE was affected by the applied voltage and by COD influent concentration, where increasing the applied voltage from 0.4 to 1.2 V at COD = 1000 mg/L, increased the CE from 9.5 ± 0.35 to 21 ± 0.5%. Moreover, increasing COD concentration from 300 mg/L to 1700 mg/L, at an applied voltage of 0.8 V, led to a decrease in coulombic efficiency from 51 ± 2.7 to 13.3 ± 0.9%. This means that a small part of the substrate was used for current generation and the rest was used for methane production (Sleutels et al., 2011). The availability of excess substrate in the anode chamber led the methanogens to consume it, instead of using it in current production. Therefore, most of COD was consumed by methanogens in long cycle duration and that led to decrease CE. In addition, current deterioration due struvite precipitation on the cathode surface decreased CE as well (Almatouq & Babatunde, 2016).

3.7 Statistical Analysis

The synthetic wastewater in this study was used to simulate reject wastewater, since reject water contains a high P concentration and can be an optimal stream for P recovery from wastewater (Wu & Modin, 2013). The results showed that the applied voltage had a great

influence on P recovery and hydrogen production. However, the impact of COD concentration on P recovery and hydrogen production was not clear. Therefore, CCD was used to find the impact of each parameter, as well as the interaction impact on MEC performance, and to identify the optimum operating conditions for the dual chamber MEC.

Theoretically, MEC requires 0.2 V to produce hydrogen gas, but in practice MEC requires > 0.2 V to produce hydrogen due to the losses (Logan et al., 2008). Furthermore, water electrolysis requires >1.2 V (in theory) to produce hydrogen (Logan et al., 2015). Therefore, the applied voltage range in this study was between (low voltage = 0.4 V) and (high voltage =1.2). The aim of the RSM is to determine the optimum and most cost effective operating conditions. Moreover, the low (COD=500 mg/L) and high (COD=1500 mg/L) levels of influent COD concentration were chosen, based on the concentration of COD in reject wastewater (Hu et al., 2017).

CCD and response surface methodology (RSM) were used to identify the impact of applied voltage (X1) and COD concentration (X2) on MEC performance, and to determine the optimum operating conditions. CCD was used to fit a quadratic model to the data. Four axials with $\alpha = \pm 1.4$ and three center points were performed to have a rotatable design. The levels of variables for CCD are given in Table 1.

The performance of the MEC was investigated in terms of cathode pH, precipitation efficiency and maximum volumetric hydrogen production rate. Cathode pH is the most important factor for P recovery, where P solubility is dependent on solution pH. Precipitation efficiency was used to evaluate P recovery as struvite in the cathode chamber. Finally, maximum volumetric hydrogen production rate was used to assess hydrogen production in MEC. The experimental design and the results are summarized in Table 1. Before finalising any model (in all responses), tests of assumptions were conducted to confirm that none of

these conditions were violated. First, the standard deviations between the actual and the predicted response values followed a normal distribution Second, the studentized residuals, versus predicted values, showed that there was no evidence for the violation of constant or independence assumptions throughout the response space. Third, check for outliers if any (influential values) are available. In these statistics, Cook's distance was used to check if there were any influential values. Last, the Box-Cox plot for power transformation was checked, to see if the data required any transformation. After all these checks, the models were finalised and the RSM was drawn up.

3.7.1 Cathode pH

Cathode pH is the most important parameter for P recovery. Cathode pH was studied to identify the impact of applied voltage and COD concentration on MEC performance. The Analysis of Variance (ANOVA) results showed that a quadratic model with an F-value of 129.44 and a P-value of <0.0001 was significant. There was only a 0.01% chance that this level of fit could occur due to noise. The lack of fit was not significant, with a P-value of 0.4487. The coefficient of determination (R^2) of 0.9818 and adjusted (R^2) of 0.9724 implied that the model was able to express approximately 98.18% of the variability in the response. The response surface of the cathode pH is shown in Fig.4-a. The following model was considered satisfactory in explaining cathode pH:

$$\text{Cathode pH} = 8.18 + 0.26\ X_1 + 0.33\ X_2 - 0.061\ X_1X_2 - 0.051\ X_1^2 - 0.11\ X_2^2 \qquad (8)$$

Table 2 shows that the effects of all terms were significant on cathode pH, except X_1^2 which was statistically insignificant. More importantly, the interaction term was significant, which means the effect of applied voltage on cathode pH is dependent on the level of COD concentration. In addition**,** Equation 8 showed that COD concentration had the greatest effect on response. The RSM graph in Fig.4-a shows that the effect of applied voltage was linear on

cathode pH and that cathode pH increased with an increase in applied voltage. However, the effect of COD concentration was quadratic on the response, and increased COD concentration increased cathode pH.

Proton consumption in the cathode chamber for hydrogen production in the MEC resulted in a pH increase. Therefore, increased COD concentration from 500 to 1500 at 1.1 V led to an increase in average cathode pH from 7.9 to 8.5. Since P solubility is dependent on solution pH, the optimal pH for struvite crystallization is 8.5 (Cusick et al., 2014). Eq .8 was able to predict a cathode pH of 8.5 at applied voltage of 1.1 V and COD concentration of 1500 mg/L. Three experimental runs were conducted to check model adequacy. A cathode pH average of 8.6 was achieved, confirming the accuracy of the model.

3.7.2 Precipitation Efficiency

Precipitation efficiency was measured to assess the P recovery efficiency of the MEC. Equation 5 was used to calculate the precipitation efficiency. The (ANOVA) results showed that quadratic model with F-value of 128.26 and P-value of < 0.0001 was significant. There was only 0.01% chance that this level of fit could occur due to noise. The lack of fit was not significant, with a P-value of 0.095. The coefficient of determination (R^2) of 0.9859 and adjusted (R^2) of 0.9782 implied that the model was able to express approximately 98.59 % of the variability in the response. The response surface of the precipitation efficiency is shown in Fig.4-b. The following model was considered satisfactory in explaining precipitation efficiency:

$$\text{Precipitation efficiency} = 90.41 + 9.45\ X_1 + 8.31\ X_2 + 2\ X_1X_2 - 11.05\ X_1^2 - 7.67\ X_2^2 + 5.69\ X_1^2X_2 \quad (9)$$

Table 2 shows that all terms were significant on precipitation efficiency, and that applied voltage had the greatest effect on precipitation efficiency. The RSM in Fig.4-b shows that the

applied voltage and COD concentration had a quadratic effect on precipitation efficiency. A low applied voltage (0.5 V) increased the COD concentration from 500 mg/L to 1500 mg/L, and also increased the precipitation efficiency from 50 to 72%. The same trend was observed at high applied voltage (1.1 V), where the precipitation efficiency increased from 62 to 95% when COD concentration increased from 500 to 1500 mg/L. Increased COD concentration increased the electrons and protons that transferred to the cathode. This, in turn, increased the catholyte pH due to proton consumption. At high pH (>8), P reached the supersaturation point. More than 90% of P can be precipitated when pH reaches 8.3 (Adnan et al., 2003). Furthermore, an increase in the applied voltage led to increased current and, as a result, to an increase in precipitation efficiency. At a low COD concentration (500 mg/L), an increase in applied voltage from 0.5 to 0.8 V increased the precipitation efficiency from 42 to 70%. However, precipitation efficiency started to decrease when applied voltage increased above 0.8 V. Increased applied voltage increased the cathode pH. By changing the applied voltage from 0.5 V to 1.1 V, the pH increased from 7.5 to 8.1, leading to an increase in ammonia volatilization and diffusion to the anode chamber (Rahman et al., 2014; Zhou & Wu, 2012) Equation 9 was able to predict a maximum precipitation efficiency of 96% at an applied voltage of 1 V, and a COD concentration of 1500 mg/L. Three experimental runs were conducted to check model adequacy. A precipitation efficiency average of 94% was achieved, and confirming the accuracy of the model.

3.7.3 Hydrogen Production Rate

The hydrogen production rate was studied to assess the ability of MEC to recover P and produce H_2. The Analysis of Variance (ANOVA) results showed that a quadratic model with an F-value of 72.28 and a P-value of < 0.0001 was significant. There was just a 0.01% chance that this level of fit could occur due to noise. The lack of fit was not significant, with a P-value of 0.6682. The coefficient of determination (R^2) of 0.9753 and adjusted (R^2) of 0.9618

implied that the model was able to express approximately 97.53% of the variability in the response. The response surface of the H_2 production rate is shown in Fig. 4-c.

The following model was considered satisfactory in explaining hydrogen production rate:

$$H_2 \text{ production rate} = 0.11 + 0.048\ X_1 - 0.024\ X_2 - 0.042\ X_1X_2 + 0.02\ X_1^2 + 2.764\times10^{-4}\ X_2^2 + 0.016\ X_1X_2^2 \quad (10)$$

Table 2 shows that the effects of all terms were significant on H_2 production rate, except X_2^2, which was statistically insignificant. More importantly, the interaction term was significant. Equation 10 shows that the effect of applied voltage had twice the effect of COD concentration on the response.

The RSM graph in Fig.4-c shows that the effects of applied voltage and COD concentration were linear and quadratic on the H_2 production rate, respectively. H_2 production increased linearly along with the applied voltage. An increase in applied voltage from 0.5 to 1.1 V increased H_2 production rate from 0.06 to 0.267 m^3-H_2/m^3-d. However, at high COD concentration (1500 mg/L) the effect of increasing applied voltage on H_2 production rate was smaller. Generally, dual chamber MECs are operated with a phosphate buffer solution (PBS) to maintain pH balance in the cathode chamber, because high cathode pH causes many losses in the system. The hydrogen production rate in this study was low, due to: (1) high internal resistance, caused by the distance between anode and cathode (8 cm). H_2 can be improved by reducing the distance (Rozendal et al., 2007), (2) substrate consumption by methanogens in high COD concentration, due to the long cycle duration, and (3) using synthetic wastewater as a catholyte instead of PBS. Using low buffer solution as a catholyte resulted in a low current, due to a limited supply of protons and high catholyte pH. Operating MEC with a high cathode pH will deteriorate the MEC performance (Nam & Logan, 2012).

The production of H_2 in low COD concentration (500 mg/L) was much better than the high COD concentration. Hydrogen production was negatively affected by the absence of a high concentration of PBS in the cathode. The change of anode and cathode pH at high COD concentration was greater than the low COD concentration. Table 3 shows that the higher the COD concentration, the higher the pH difference between anode and cathode chambers, and the less H_2 production in MEC. This explains why the production of H_2 was low (Rivera et al., 2015; Yossan et al., 2013). A high pH difference between anode and cathode chambers led to high potential losses, negatively affecting MEC performance. Thus, PBS was used in most of the dual chamber MECs to maintain the pH balance during the operation of the system (Luo et al., 2014).

4.0 Conclusion

Phosphorus was efficiently precipitated as struvite in the cathode chamber of mediator-less dual chamber microbial electrolysis cell. The MEC achieved a maximum H_2 production rate of 0.28 m^3-H_2/m^3-d (at applied voltage = 1.1 V , COD = 500 mg/L) and a maximum precipitation efficiency of 95 % (at applied voltage =1.1 applied voltage, COD =1500 mg/L). Cathode and membrane scaling, as well as high pH difference between anode and cathode led to a deterioration in MEC performance. The produced H_2 in MEC can be used as an energy source to reduce struvite operational cost.

Acknowledgments

The Authors would like to acknowledge the technical staff at the Cardiff University School of Engineering for supporting them. The first author would like to thank Kuwait Institute for Scientific Research for their financial support.

Conflicts of Interest: The authors declare no conflict of interest.

This research did not receive any specific grant from funding agencies in the public, commercial, or not-for-profit sectors.

References

1) Adnan, A., Koch, F.A., Mavinic, D.S. 2003. Pilot-scale study of phosphorus recovery through struvite crystallization-II: Applying in-reactor supersaturation ratio as a process control parameter. *Journal of Environmental Engineering and Science*, **2**(6), 473-483.
2) Almatouq, A., Babatunde, A.O. 2016. Concurrent Phosphorus Recovery and Energy Generation in Mediator-Less Dual Chamber Microbial Fuel Cells: Mechanisms and Influencing Factors. *International Journal of Environmental Research and Public Health*, **13**(4), 375.
3) Call, D., Logan, B.E. 2008. Hydrogen production in a single chamber microbial electrolysis cell lacking a membrane. *Environmental science & technology*, **42**(9), 3401-3406.
4) Çelen, I., Buchanan, J.R., Burns, R.T., Robinson, R.B., Raman, D.R. 2007. Using a chemical equilibrium model to predict amendments required to precipitate phosphorus as struvite in liquid swine manure. *Water Research*, **41**(8), 1689-1696.
5) Çetinkaya, A.Y., Köroğlu, E.O., Demir, N.M., Baysoy, D.Y., Özkaya, B., Çakmakçı, M. 2015. Electricity production by a microbial fuel cell fueled by brewery wastewater and the factors in its membrane deterioration. *Chinese Journal of Catalysis*, **36**(7), 1068-1076.
6) Cooper, J., Lombardi, R., Boardman, D., Carliell-Marquet, C. 2011. The future distribution and production of global phosphate rock reserves. *Resources, Conservation and Recycling*, **57**, 78-86.
7) Cord-Ruwisch, R., Law, Y., Cheng, K.Y. 2011. Ammonium as a sustainable proton shuttle in bioelectrochemical systems. *Bioresource technology*, **102**(20), 9691-9696.
8) Cusick, R.D., Logan, B.E. 2012. Phosphate recovery as struvite within a single chamber microbial electrolysis cell. *Bioresource technology*, **107**, 110-115.
9) Cusick, R.D., Ullery, M.L., Dempsey, B.A., Logan, B.E. 2014. Electrochemical struvite precipitation from digestate with a fluidized bed cathode microbial electrolysis cell. *water research*, **54**, 297-306.
10) Ding, A., Yang, Y., Sun, G., Wu, D. 2016. Impact of applied voltage on methane generation and microbial activities in an anaerobic microbial electrolysis cell (MEC). *Chemical Engineering Journal*, **283**, 260-265.
11) Doyle, J.D., Parsons, S.A. 2002. Struvite formation, control and recovery. *Water research*, **36**(16), 3925-3940.
12) Fattah, K.P., Mavinic, D.S., Koch, F.A., Jacob, C. 2008. Determining the feasibility of phosphorus recovery as struvite from filter press centrate in a secondary wastewater treatment plant. *Journal of Environmental Science and Health, Part A*, **43**(7), 756-764.
13) Hu, D., Zhou, Z., Niu, T., Wei, H., Dou, W., Jiang, L.-M., Lv, Y. 2017. Co-treatment of reject water from sludge dewatering and supernatant from sludge lime stabilization process for nutrient removal: A cost-effective approach. *Separation and Purification Technology*, **172**, 357-365.
14) Hutnik, N., Piotrowski, K., Wierzbowska, B., Matynia, A. 2011. Continuous reaction crystallization of struvite from phosphate (V) solutions containing calcium ions. *Crystal Research and Technology*, **46**(5), 443-449.
15) Jaffer, Y., Clark, T., Pearce, P., Parsons, S. 2002. Potential phosphorus recovery by struvite formation. *Water Research*, **36**(7), 1834-1842.
16) Kuntke, P., Sleutels, T., Saakes, M., Buisman, C. 2014. Hydrogen production and ammonium recovery from urine by a Microbial Electrolysis Cell. *International Journal of Hydrogen Energy*, **39**(10), 4771-4778.
17) Logan, B.E., Call, D., Cheng, S., Hamelers, H.V., Sleutels, T.H., Jeremiasse, A.W., Rozendal, R.A. 2008. Microbial electrolysis cells for high yield hydrogen gas production from organic matter. *Environmental Science & Technology*, **42**(23), 8630-8640.

18) Logan, B.E., Wallack, M.J., Kim, K.-Y., He, W., Feng, Y., Saikaly, P.E. 2015. Assessment of microbial fuel cell configurations and power densities. *Environmental Science & Technology Letters*, **2**(8), 206-214.
19) Luo, H., Liu, G., Zhang, R., Bai, Y., Fu, S., Hou, Y. 2014. Heavy metal recovery combined with H 2 production from artificial acid mine drainage using the microbial electrolysis cell. *Journal of hazardous materials*, **270**, 153-159.
20) Morales, N., Boehler, M.A., Buettner, S., Liebi, C., Siegrist, H. 2013. Recovery of N and P from urine by struvite precipitation followed by combined stripping with digester sludge liquid at full scale. *Water*, **5**(3), 1262-1278.
21) Moussa, S.B., Maurin, G., Gabrielli, C., Amor, M.B. 2006. Electrochemical precipitation of struvite. *Electrochemical and solid-state letters*, **9**(6), C97-C101.
22) Nam, J.-Y., Logan, B.E. 2012. Optimization of catholyte concentration and anolyte pHs in two chamber microbial electrolysis cells. *international journal of hydrogen energy*, **37**(24), 18622-18628.
23) Pasupuleti, S.B., Srikanth, S., Mohan, S.V., Pant, D. 2015. Development of exoelectrogenic bioanode and study on feasibility of hydrogen production using abiotic VITO-CoRE™ and VITO-CASE™ electrodes in a single chamber microbial electrolysis cell (MEC) at low current densities. *Bioresource technology*, **195**, 131-138.
24) Rahman, M.M., Salleh, M.A.M., Rashid, U., Ahsan, A., Hossain, M.M., Ra, C.S. 2014. Production of slow release crystal fertilizer from wastewaters through struvite crystallization–A review. *Arabian Journal of Chemistry*, **7**(1), 139-155.
25) Rivera, I., Buitrón, G., Bakonyi, P., Nemestóthy, N., Bélafi-Bakó, K. 2015. Hydrogen production in a microbial electrolysis cell fed with a dark fermentation effluent. *Journal of Applied Electrochemistry*, **45**(11), 1223-1229.
26) Ronteltap, M., Maurer, M., Hausherr, R., Gujer, W. 2010. Struvite precipitation from urine–influencing factors on particle size. *Water research*, **44**(6), 2038-2046.
27) Rozendal, R.A., Hamelers, H.V., Molenkamp, R.J., Buisman, C.J. 2007. Performance of single chamber biocatalyzed electrolysis with different types of ion exchange membranes. *Water Research*, **41**(9), 1984-1994.
28) Ruiz, Y., Baeza, J.A., Guisasola, A. 2015. Enhanced performance of bioelectrochemical hydrogen production using a pH control strategy. *ChemSusChem*, **8**(2), 389-397.
29) Sleutels, T.H., Darus, L., Hamelers, H.V., Buisman, C.J. 2011. Effect of operational parameters on Coulombic efficiency in bioelectrochemical systems. *Bioresource technology*, **102**(24), 11172-11176.
30) Tao, Q., Luo, J., Zhou, J., Zhou, S., Liu, G., Zhang, R. 2014. Effect of dissolved oxygen on nitrogen and phosphorus removal and electricity production in microbial fuel cell. *Bioresource technology*, **164**, 402-407.
31) Wu, X., Modin, O. 2013. Ammonium recovery from reject water combined with hydrogen production in a bioelectrochemical reactor. *Bioresource technology*, **146**, 530-536.
32) Xu, J., Sheng, G.-P., Luo, H.-W., Li, W.-W., Wang, L.-F., Yu, H.-Q. 2012. Fouling of proton exchange membrane (PEM) deteriorates the performance of microbial fuel cell. *water research*, **46**(6), 1817-1824.
33) Yossan, S., Xiao, L., Prasertsan, P., He, Z. 2013. Hydrogen production in microbial electrolysis cells: choice of catholyte. *international journal of hydrogen energy*, **38**(23), 9619-9624.
34) You, J., Greenman, J., Melhuish, C., Ieropoulos, I. 2015. Electricity generation and struvite recovery from human urine using microbial fuel cells. *Journal of Chemical Technology and Biotechnology*.
35) Zhou, S., Wu, Y. 2012. Improving the prediction of ammonium nitrogen removal through struvite precipitation. *Environmental Science and Pollution Research*, **19**(2), 347-360.

No of run	Block	X_1: Applied voltage (V)	X_2: COD (mg/L)	Y_1: cathode pH	Y_2: Precipitation efficiency (%)	Y_3: Max volumetric H_2 production (m^3-H_2/m^3-d)
1	Block 1	0.5	500	7.43	50	0.06025
2	Block 1	0.5	1500	8.25	70	0.08514
3	Block 1	1.1	1500	8.47	91	0.1318
4	Block 1	1.1	500	7.95	62	0.28057
5	Block 1	0.5	500	7.4	44	0.061
6	Block 1	1.1	1500	8.67	95	0.13987
7	Block 1	0.8	1000	8.25	90	0.10052
8	Block 1	1.1	500	8.067	60	0.2674
9	Block 1	0.8	1000	8.24	88	0.13101
10	Block 1	0.5	1500	8.189	72	0.09755
11	Block 2	0.4	1000	7.7	57	0.076
12	Block 2	0.8	300	7.44	68	0.15939
13	Block 2	1.2	1000	8.49	87	0.20943
14	Block 2	0.8	1700	8.4	91	0.06564
15	Block 2	1.2	1000	8.4	85	0.22482
16	Block 2	0.8	1000	8.1	90	0.11677
17	Block 2	0.8	1700	8.35	90	0.09103
18	Block 2	0.4	1000	7.6	59	0.08678
19	Block 2	0.8	300	7.5	66	0.1223

Source	Sum of Squares	DF	Mean Square	F-Value	P-value
Cathode pH					
Block	0.042	1	0.042		
Model	2.95	5	0.59	129.44	< 0.0001
X_1	1.07	1	1.07	234.82	< 0.0001
X_2	1.75	1	1.75	384.28	< 0.0001
X_1X_2	0.030	1	0.030	6.48	0.0256
X_1^2	0.020	1	0.020	4.32	0.0597
X_2^2	0.098	1	0.098	21.45	0.0006
Residual	0.055	12	4.554E-003		
Lack of Fit	0.013	3	4.449E-003	0.97	0.4487
Pure Error	0.041	9	4.589E-003		
Total	3.04	18			
Precipitation efficiency					
Block	109.14	1	109.14		
Model	4544.64	6	757.44	128.26	< 0.0001
X_1	1428.76	1	1428.76	241.94	< 0.0001
X_2	552.25	1	552.25	93.52	< 0.0001
X_1X_2	32.00	1	32.00	5.42	0.0400
X_1^2	927.00	1	927.00	156.97	< 0.0001
X_2^2	447.18	1	447.18	75.72	< 0.0001
$X_1^2 X_2$	129.57	1	129.57	21.94	0.0007
Residual	64.96	11	5.91		
Lack of Fit	26.46	2	13.23	3.09	0.0950
Pure Error	38.50	9	4.28		
H_2 production rate					
Block	2.660E-004	1	2.660E-004		
Model	0.080	6	0.013	72.28	< 0.0001
X_1	0.018	1	0.018	100.27	< 0.0001
X_2	9.588E-003	1	9.588E-003	52.18	< 0.0001
X_1X_2	0.014	1	0.014	77.60	< 0.0001
X_1^2	3.071E-003	1	3.071E-003	16.71	0.0018
X_2^2	5.800E-007	1	5.800E-007	3.157E-003	0.9562
$X_1 X_2^2$	1.085E-003	1	1.085E-003	5.91	0.0334
Residual	2.021E-003	11	1.838E-004		
Lack of Fit	1.732E-004	2	8.660E-005	0.42	0.6682
Pure Error	1.848E-003	9	2.053E-004		
Total	0.082	18			

COD concentration (mg/L)	Cathode pH	Anode pH	ΔpH
500	7.98 ± 0.11	6.84 ± 0.04	1.1 ± 0.1
1000	8.17 ± 0.09	6.34 ± 0.06	1.8 ± 0.2
1500	8.43 ± 0.12	6.35 ± 0.03	2.1 ± 0.2

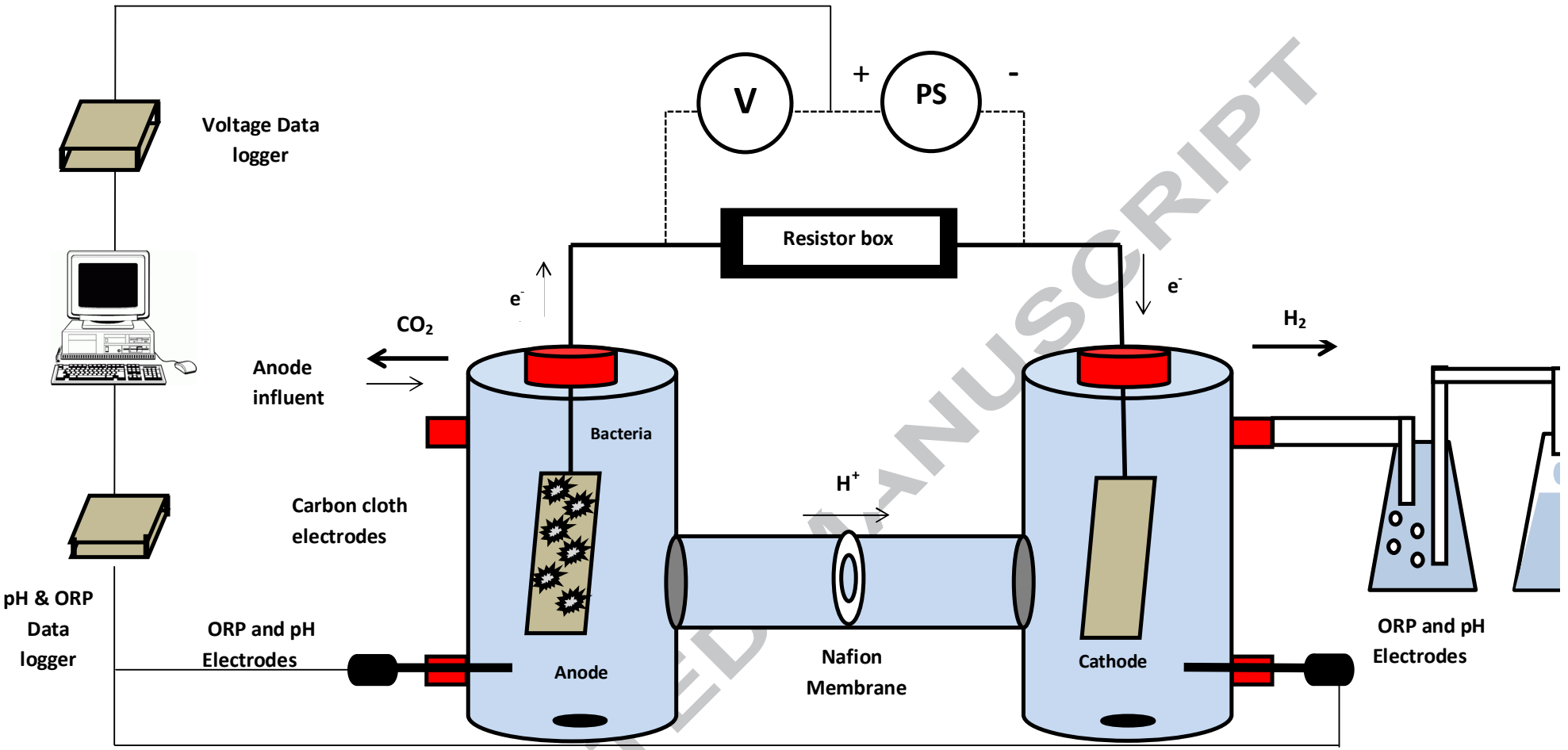

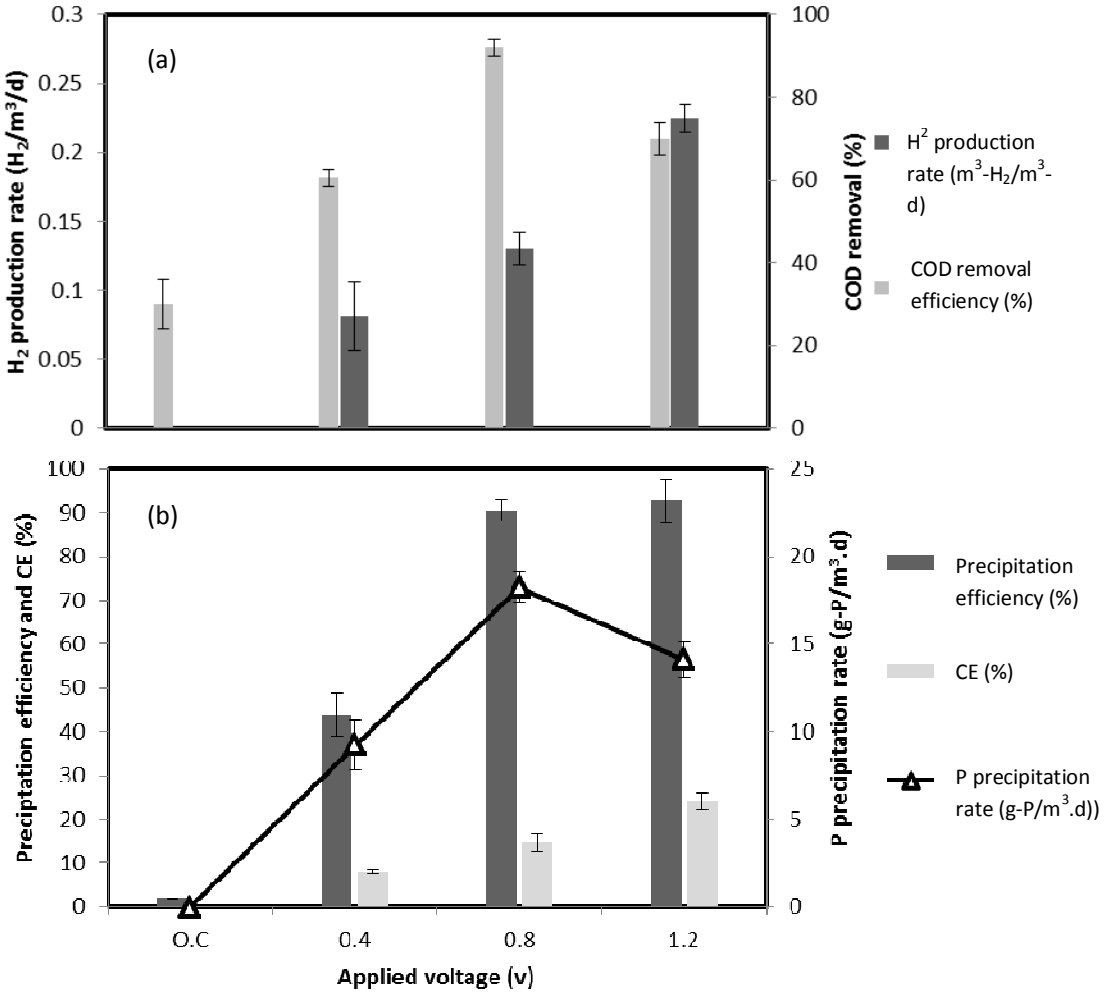

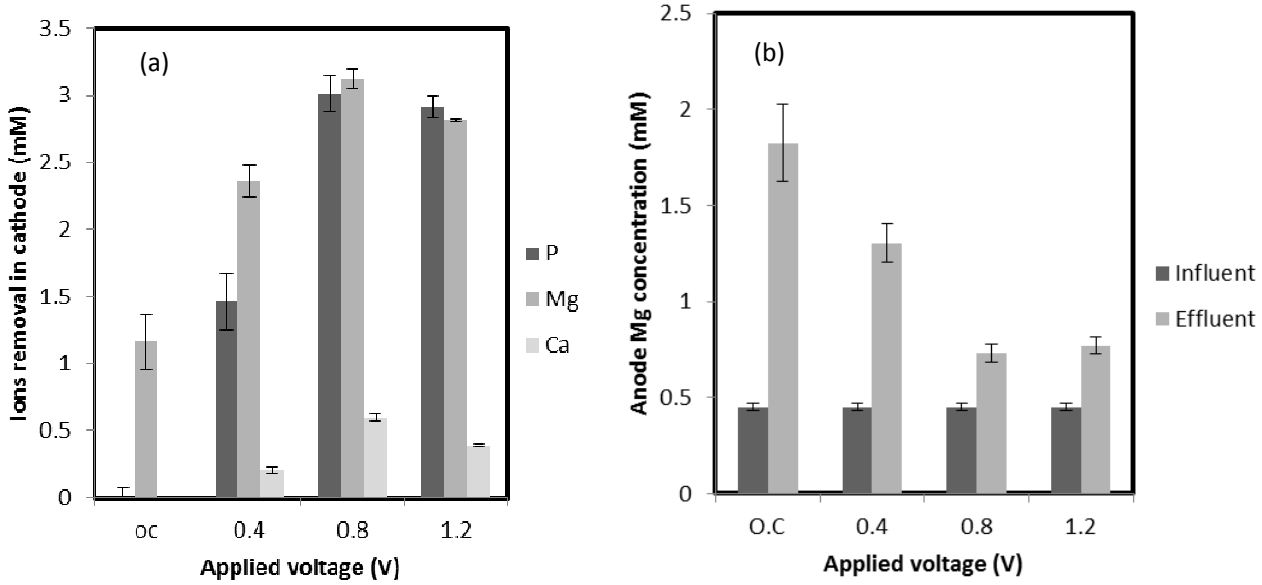

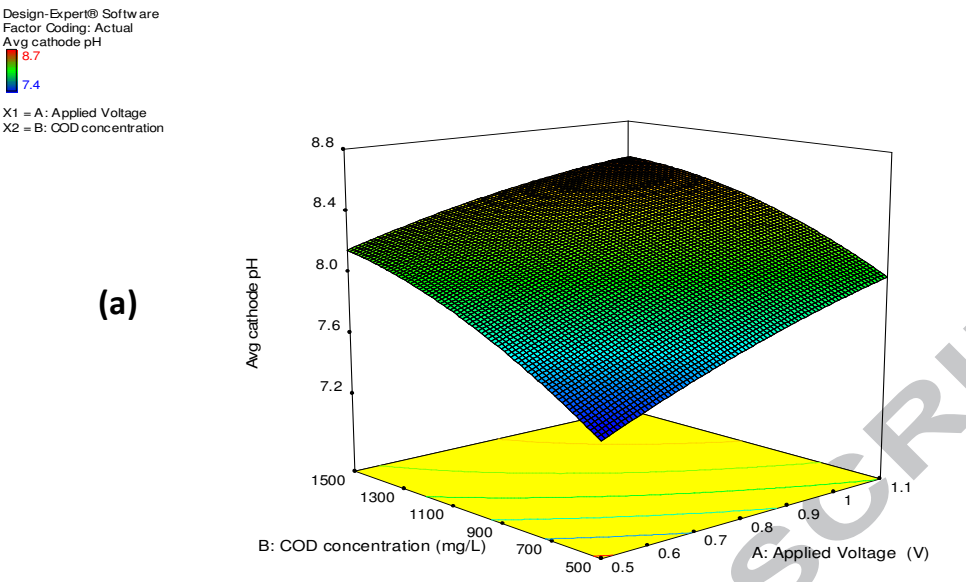

(a)

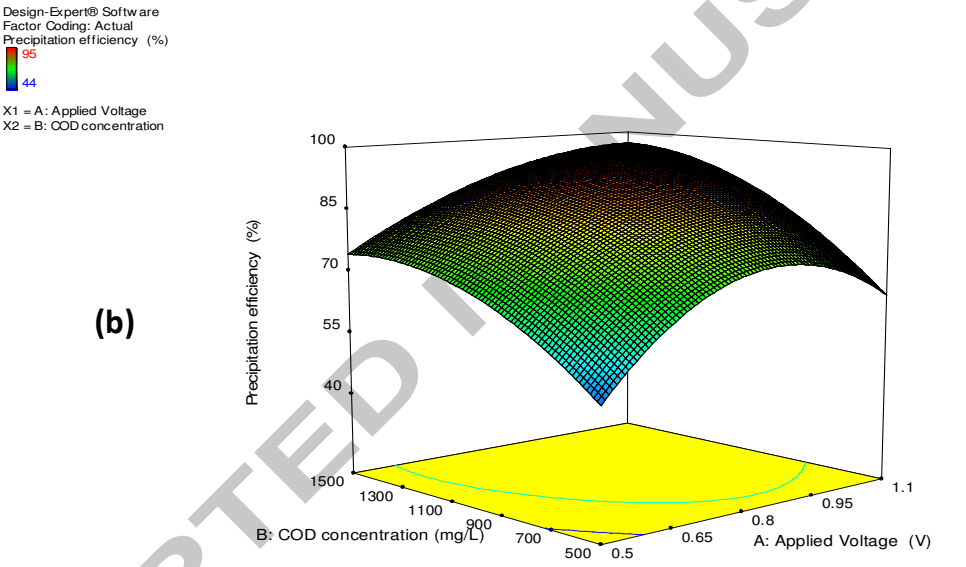

(b)

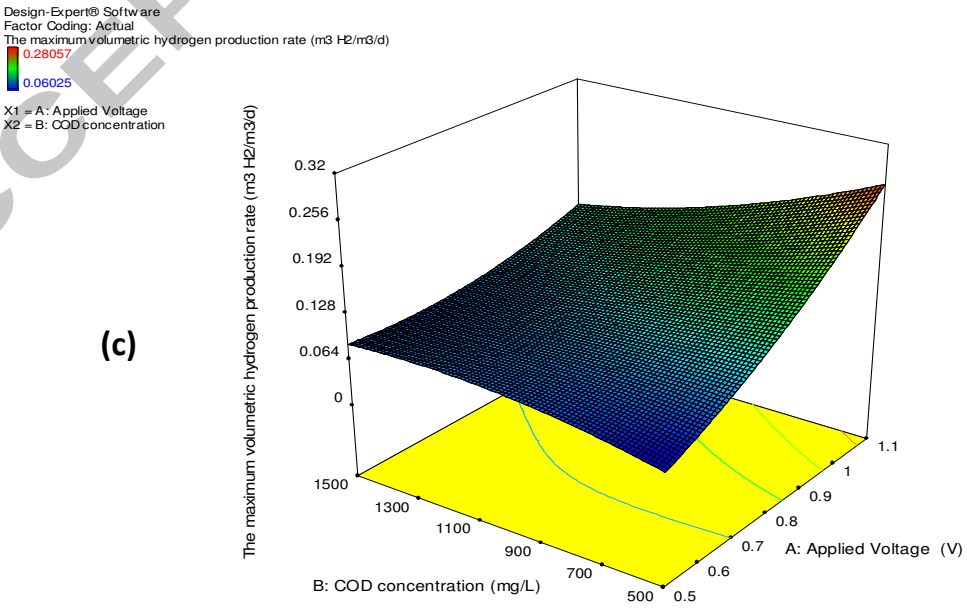

(c)

Highlights

- Phosphorus was recovered as struvite in the cathode chamber of the MEC.
- The applied voltage had a great influence on H_2 production rate and P recovery.
- COD concentration influenced P recovery only.
- Overall energy recoveries in the MEC ranged from η_{E+S}= 25 ± 1 % to 37 ± 1.7 %